

Contents lists available at [SciVerse ScienceDirect](#)

Icarus

journal homepage: www.elsevier.com/locate/icarus

Isotopic and geochemical investigation of two distinct Mars analog environments using evolved gas techniques in Svalbard, Norway

Jennifer C. Stern^{a,*}, Amy C. McAdam^a, Inge L. Ten Kate^{a,b}, David L. Bish^c, David F. Blake^d, Richard V. Morris^e, Roxane Bowden^f, Marilyn L. Fogel^f, Mihaela Glamoclija^f, Paul R. Mahaffy^a, Andrew Steele^f, Hans E.F. Amundsen^g

^a Planetary Environments Laboratory, Code 699, NASA Goddard Space Flight Center, Greenbelt, MD 20910, USA

^b Centre for Physics of Geological Processes, University of Oslo, 0316 Oslo, Norway

^c Department of Geological Sciences, Indiana University, Bloomington, IN 47405, USA

^d Exobiology Branch, MS 239-4, NASA Ames Research Center, Moffett Field, CA 94035, USA

^e Astromaterials Branch, NASA Johnson Space Center, Houston, TX 77058, USA

^f Geophysical Laboratory, Carnegie Institute of Washington, Washington, DC 20015, USA

^g Earth and Planetary Exploration Services, Oslo, Norway

ARTICLE INFO

Article history:

Available online xxxxx

ABSTRACT

The 2010 Arctic Mars Analog Svalbard Expedition (AMASE) investigated two distinct geologic settings on Svalbard, using methodologies and techniques to be deployed on Mars Science Laboratory (MSL). AMASE-related research comprises both analyses conducted during the expedition and further analyses of collected samples using laboratory facilities at a variety of institutions. The Sample Analysis at Mars (SAM) instrument suite on MSL includes pyrolysis ovens, a gas-processing manifold, a quadrupole mass spectrometer (QMS), several gas chromatography columns, and a Tunable Laser Spectrometer (TLS). An integral part of SAM development is the deployment of SAM-like instrumentation in the field. During AMASE 2010, two parts of SAM participated as stand-alone instruments. A Hidden Evolved Gas Analysis-Mass Spectrometer (EGA-QMS) system represented the EGA-QMS component of SAM, and a Picarro Cavity Ring Down Spectrometer (EGA-CRDS), represented the EGA-TLS component of SAM. A field analog of CheMin, the XRD/XRF on MSL, was also deployed as part of this field campaign. Carbon isotopic measurements of CO₂ evolved during thermal decomposition of carbonates were used together with EGA-QMS geochemical data, mineral composition information and contextual observations made during sample collection to distinguish carbonates formation associated with chemosynthetic activity at a fossil methane seep from abiotic processes forming carbonates associated with subglacial basaltic eruptions. Carbon and oxygen isotopes of the basalt-hosted carbonates suggest cryogenic carbonate formation, though more research is necessary to clarify the history of these rocks.

Published by Elsevier Inc.

1. Introduction

Terrestrial analogs of Mars and other planetary bodies provide a valuable opportunity for studying environments and processes inaccessible to us due the remote nature of these places (Léveillé, 2009). Additionally, these places are testing and proving grounds for scientific instrumentation to be deployed on planetary missions. Mars analog studies have been conducted in the Atacama and Mojave Deserts, lakes in Antarctica, and the Rio Tinto river in Spain (Bishop et al., 2001, 2011; Fernandez-Remolar et al., 2005; Navarro-Gonzalez et al., 2004, 2003). These different sites are analogous to environments on Mars at various points in its

environmental and geological history. These studies have revealed much regarding the form that life might have taken in analogous Mars environments, and the limits of habitability. But they have also been used to test instrumentation and interpret results of missions (e.g. Viking, (Navarro-Gonzalez et al., 2010)).

The Arctic Mars Analog Svalbard Expedition (AMASE) has been funded by NASA's Astrobiology Science and Technology for Exploring Planets (ASTEP) Program to study Mars analog sites on Spitsbergen Island, Svalbard, Norway since 2003. Svalbard is an island archipelago with a range of geochemical conditions and geological formations. Some of the most studied of these formations are carbonate-encrusted volcanic vents hosting carbonates that bear a striking resemblance to the carbonate globules in martian meteorite ALH84001. These carbonates are thought to have been deposited in association with subglacial basaltic volcanism (Steele

* Corresponding author. Fax: +1 301 614 6406.

E-mail address: Jennifer.C.Stern@nasa.gov (J.C. Stern).

et al., 2007; Treiman et al., 2002). Such processes have been envisioned on Mars to invoke the presence of liquid water and subsequent precipitation of carbonate cements, e.g. Comanche carbonates discovered from MER (A) data in Morris et al. (2010, 2011).

The past several AMASE campaigns have assembled an international team with a powerful suite of instruments to simulate methodologies and techniques in use or development for existing or proposed Mars landed missions such as Mars Science Laboratory (MSL), ExoMars, and Mars Sample Return (MSR). Using the capabilities a rover with these instruments would have, the AMASE team makes geochemical, mineralogical, and biological measurements in the field. After the field campaign, the same samples are analyzed by state of the art technology at the given instrument's home institution to ground truth field measurements. Some experiments are direct life detection experiments, but most address characterization of habitability and biosignatures. Because this is an astrobiology study, the emphasis is placed on the question of whether the AMASE instrument suite can distinguish biological from abiotic processes at these Mars analog sites.

Relative to its earlier campaigns, AMASE 2010 had a new field capability to assist in this mission – the ability to measure the carbon stable isotopic composition ($\delta^{13}\text{C}$) of solid materials using evolved gas analysis and custom front end coupled with a commercially available Cavity Ring Down Spectrometer (Picarro CO_2 Isotope Analyzer). Stable isotopes are powerful tracers of biological and geochemical processes on Earth. The magnitude and the direction (positive or negative) of isotopic fractionation between different isotopes of the same element can fingerprint the source and mechanism associated with its transformation. For example, photosynthesis leads to preferential enrichment of the light isotope of carbon (i.e., ^{12}C) in its products, resulting in negative $\delta^{13}\text{C}$ values relative to atmospheric CO_2 (Farquhar et al., 1989; Hayes, 1993; Hoefs, 1980). In contrast, the precipitation of carbonate results in a positive fractionation with respect to the atmosphere. This is why organics associated with biological processes on Earth have $\delta^{13}\text{C}$ values distinct from those of atmospheric and geological carbon reservoirs.

It is plausible that similar fractionation between biological and geological carbon could occur on Mars. Although the pathways and mechanisms for the cycling of carbon on Mars are largely unknown, any life would require exchange of energy and resources with its environment. The chemical reactions governing that exchange are likely to be based on universal laws of physics, in which different isotopic species have different reaction rates related to their Gibbs Free Energy (O'Neil, 1986). Thus, metabolic processing of carbon on Mars should produce isotopic fractionation analogous to the kinetic isotope effect induced by enzyme-mediated carboxylation to assimilate CO_2 , producing changes in $^{13}\text{C}/^{12}\text{C}$ that can be traced in the sedimentary record (Schidlowski, 1992). There are caveats associated with using $\delta^{13}\text{C}$ as a biosignature, particularly studies in the past 10 years showing that organic carbon compounds produced by abiotic processes may have the same ^{13}C fractionation as biologic carbon (e.g. McCollom and Seewald, 2006). Studies to determine sources of methane in hydrothermal environments on Earth (e.g. Lost City Hydrothermal System) have shown a wide range of $\delta^{13}\text{C}$ values for abiotic methane that overlap biologically and thermogenically produced methane (Proskurowski et al., 2006; Sherwood-Lollar et al., 2008). Hydrothermal activity has been suggested to have occurred on Mars (Schulze-Makuch et al., 2007), such as that induced by impacts early in its history (Abramov and Kring, 2005) and could therefore have been a source of abiotic fractionation on Mars as well. In addition, abiotic organics with $\delta^{13}\text{C} = -5\text{‰}$ to -20‰ from carbonaceous chondrites are likely to be present on the martian surface (Huang et al., 2005; Sephton et al., 2003). Thus, discovery of ^{13}C -depleted carbon,

particularly when not in context with the inorganic carbon source (e.g. contemporaneous carbonates) does not alone indicate biological activity. Nevertheless, because of their potential as biosignatures, stable isotope compositions of Mars atmosphere and surface materials are high priority measurements as defined by the Mars Exploration Program Assessment Group (MEPAG Science Goals, Objectives, Investigations, and Priorities: 2010) as well as the National Academies Planetary Science Decadal Survey Report for 2013–2022 (2011).

We know relatively little about the isotopic composition of carbon on Mars, although detailed isotopic studies of carbonates in martian meteorites of different ages may help to interpret future *in situ* isotopic measurements of carbonates in regolith. The $\delta^{13}\text{C}$ of modern atmospheric CO_2 on Mars, as measured by Mars Phoenix (Niles et al., 2010) is thought to be lighter than CO_2 on ancient Mars, assuming the atmospheric reservoir of CO_2 is recorded in carbonate from martian meteorites. The oldest meteorites have the heaviest $\delta^{13}\text{C}$, suggesting atmospheric loss of ^{12}C on early Mars (Carr et al., 1985; Jakosky, 1999; Jull et al., 1997; Wright et al., 1988). Together, the discovery of temporal variations of methane on Mars (Mumma et al., 2009; Villanueva et al., 2009) and the identification of carbonates by Phoenix, CRISM, TES, and mini-TES (Boynton et al., 2009; Ehlmann et al., 2008; Morris et al., 2010), suggest that at least 3 carbon species exist on Mars (CO_2 , CH_4 , and carbonates). $\delta^{13}\text{C}$ measurements of these three reservoirs are achievable with the MSL instrument suite, as well as $\delta^{13}\text{C}$ of organic carbon, should it be present. While these values alone will be difficult to interpret without contextual information, the instrument suite on MSL is capable of obtaining mineralogical and geochemical data along with high-resolution imaging that may provide a framework for the interpretation of isotopic data.

1.1. Brief overview of the AMASE 2010 campaign

The 2010 AMASE campaign was based in Ny Ålesund, the northernmost permanently inhabited community in the world at $78^\circ 55'\text{N}$ $11^\circ 56'\text{E}$, and carried an unprecedented array of instrumentation for geochemical characterization, life detection, and high resolution imaging of the Mars analog field sites. The 2010 campaign was comprised of 33 people and 8 instruments (Table 1): SAM (Mahaffy, 2008), CheMin (Blake et al., 2010), PanCam (Amundsen et al., 2010), MOMA (Goetz et al., 2011), Raman/LIBS (Rull et al., 2011), SPDS Rock Crusher, CLUPI (Josset et al., 2011), and VAPoR (ten Kate et al., 2010). This year's campaign focused on two sites, described below. These sites were visited by a small team of field

Table 1
AMASE 2010 instrument payload.

Instrument	Team	Capability
CheMin	Blake/ Morris	Powder XRD and XRF
CLUPI	Josset/ Josset	Imaging, high resolution
MOMA	Philippon/ Steinmetz	Gas chromatography
PanCam	Schmitz/ Cousins/ Bauer	Imaging, panoramic, stereo, and multispectral
Compass Raman spectrometer, portable LIBS	Sansano/ Lopez	Raman spectrometer, laser induced breakdown spectroscopy
SAM	Stern/ McAdam	Evolved Gas Analysis Mass Spectrometry (EGA-MS), $\delta^{13}\text{C}$ via Cavity Ring Down Spectroscopy (CRDS)
SPDS crushing station	Viscor	Sample preparation, rock crusher
VAPoR	Ten Kate	Pyrolysis mass spectrometry

scientists who imaged the sites using PanCam and took field notes. This team collected a range of samples that were further imaged using CLUPI. The samples were then brought back to Ny Ålesund and presented to the Ny Ålesund-based scientists who decided which samples to analyze based on the PanCam and CLUPI imaging, field notes, and scientific priority. Samples designated for analysis were either crushed with the SPDS Rock Crusher (an engineering model of the rock crusher designed for the ExoMars mission), crushed manually using a mortar and pestle, or removed from a surface or interface using a dremel tool, and subsequently distributed to the SAM, CheMin, MOMA, and VAPoR instruments.

1.2. Mars Science Laboratory

Our approach focuses on evaluating the capability of a subset of instrumentation that will fly on the Mars Science Laboratory (MSL), “Curiosity,” to characterize two distinct environments, with the intention of distinguishing geochemical and biogeochemical processes. MSL will land on Mars in August 2012 and deploy a diverse instrument payload that will perform chemical, isotopic, and mineralogical analyses to assess the past and present potential habitability of a target environment on Mars. Our field instrumentation represents custom modification of commercially available instruments to simulate several capabilities of Sample Analysis at Mars (SAM, PI Mahaffy; Mahaffy, 2008; Mahaffy et al., 2012), and the Chemistry and Mineralogy (CheMin, PI Blake; Blake et al., 2010) experiment.

SAM (Mahaffy et al., 2012) consists of a quadrupole mass spectrometer (QMS), a gas chromatograph (GC), and a tunable laser mass spectrometer (TLS), all of which analyze gases evolved during pyrolysis or combustion of surface materials. SAM's pyrolysis ovens will heat samples to ~1000 °C with helium carrier gas. The evolved gas may be sampled directly by the QMS, or it may be routed to a hydrocarbon trap, one of six gas chromatography columns, or the TLS, for isotopic analysis (Mahaffy et al., 2012; Webster, 2005; Webster and Mahaffy, 2011). In support of SAM, an array of laboratory work with relevant Mars analog materials is being carried out at NASA's Goddard Space Flight Center (GSFC).

CheMin is an X-ray Diffraction (XRD) and X-ray Fluorescence (XRF) instrument that will measure the mineralogical (quantitative) and elemental (qualitative) composition of powdered rock or soil samples, which will help characterize the environmental and geological context of the setting. CheMin detection limits are stated to be better than 3% by mass, an accuracy of better than 15% and a precision of better than 10% of the amount present for phases present in concentrations >4X the minimum detection limit (12%) (Blake et al., 2010). CheMin and SAM EGA-QMS experiments are complementary, as identifying gases evolved from thermal decomposition of samples can help fingerprint mineral phases.

This paper focuses on how the solid sample analysis capabilities characteristic of SAM and CheMin, were used to address the origin of carbon of two distinct analog environments. We present data collected using a subset of the capabilities available on MSL, focusing on SAM evolved gas analysis, SAM TLS analysis of CO₂ from carbonates, and bulk mineralogical data from CheMin. Both EGA-QMS and CheMin provide mineralogical and environmental context crucial for interpretation of isotope data. Here we present mineralogical, geochemical, and carbon isotopic evidence of possible relict biological activity at a fossil methane seep, as well as abiotic carbonate formation through hydrothermal mechanisms at two separate sites on Spitsbergen Island, Svalbard, using methods analogous to those available on the SAM instrument suite and the CheMin experiment on the Mars Science Laboratory “Curiosity.” Our results are comparable to measurements made by laboratory isotope ratio mass spectrometry (IRMS) and demonstrate the utility of stable isotopes as tracers of relict biological activity when coupled with contextual mineralogical and environmental information.

1.3. Site description

Two sites on Spitsbergen Island, the largest of the islands comprising the Svalbard Archipelago, were chosen for their potential similarity to environments that may once have existed on Mars. Sigurdffjell is part of the Quaternary Bockfjorden Volcanic Complex (BVC) characterized by coarse pyroclastics, mantle xenoliths, and volcanic vents (Skjelkvale et al., 1989). These basalts were erupted into a thick ice cap 1 Ma ago. The vents are encrusted with carbonates that are suggested to have been precipitated from hydrothermal waters (Treiman et al., 2002). These carbonates have been found in globules very similar to carbonate globules in martian meteorite ALH84001, also formed by aqueous processes (Halevy et al., 2011; Niles et al., 2009; Steele et al., 2007). Another similarity to Mars geology is inherent in the formation of the Sigurdffjell volcanic rocks by direct eruption into ice, similar to putative volcanism on Mars, which would have melted ice and enabled hydrothermal systems (Chapman and Tanaka, 2002; Edwards et al., 2009; Hamilton et al., 2011).

The fossil methane seeps at Knorringfjell are comprised of Jurassic marine shale and carbonate mounds. These seeps, which are close to the Jurassic–Cretaceous boundary in age, are part of the Slottsmøya Member of the Agardhfjellet Formation, a well-studied sedimentary body deposited under open marine shelf conditions spanning 20 myr (e.g. Dypvik et al., 1991a, 1991b; Hammer et al., 2011; Nagy and Basov, 1998). The Slottsmøya Member is characterized by black mudstones containing macroscopic fossils of benthic organisms along with siderite and dolomite cements (Hammer et al., 2011; Krajewski, 2004; Nakrem et al., 2010). The petrography of seep carbonates has been well characterized, and these samples contain a heterogeneous mixture of black micrite, fossil-rich wackestone, brown to yellow calcite crusts, fibrous calcite, and calcite spar (Hammer et al., 2011).

Massive carbonates have not been identified on the martian surface, and acidic conditions thought to be present in the Noachian would preclude their formation (Fairen et al., 2005). However, shallow marine sediments associated with methane seeps representing chemolithotrophic ecosystems, such as those present in fossilized form at Knorringfjell, are an analog for one possible biological community that may have been preserved in shallow marine sediments during the Noachian on Mars (Fairen et al., 2005; Komatsu and Ori, 2000; Parnell et al., 2002). Fossil methane seeps have also been associated with the presence of methane hydrates, which have been suggested as sources of methane to the martian atmosphere (Komatsu et al., 2011). In addition, landforms on the martian surface have been interpreted as mud volcanoes, and terrestrial mud volcanoes are often associated with pressurized methane gas (Pondrelli et al., 2011).

2. Methods and procedure

2.1. Sample collection and preparation

Samples were collected at the field sites to the highest standards of organic cleanliness possible, using a rock hammer to break rocks to expose a fresh surface, collection with gloves, and immediate storage of sample in ashed (500 °C overnight) aluminum foil. At Knorringfjell, samples were collected from float (surface rocks assumed to have been broken off from the local host bedrock). For Terra analyses, sample chunks were crushed using the prototype SPDS Rock Crusher. In between samples, fused silica was processed through the rock crusher to remove the previous sample and prevent cross contamination. Samples were then ground to a powder of ~150 μm consistent with the grain size that the Sample Acquisition, Processing, and Handling (SA/SPaH) subsystem will

deliver to SAM and CheMin on MSL. For the SAM-like EGA-QMS and isotopic analyses, sample chips were hand-ground to a powder using an agate mortar and pestle to avoid possible organic contamination from the SPDS Rock Crusher. The CLOSe Up Imager (CLUPI) team provided context imagery for samples.

2.2. Remote laboratory/field instrumentation

During AMASE 2010, a Terra XRD/XRF (analogous to CheMin) and two components of SAM were deployed as stand-alone instruments in a remote temporary laboratory at Ny Ålesund. An in-house pyrolysis oven coupled with a Hiden Analytical HPR-20 quadrupole mass spectrometer (Fig. 1) represented the EGA-QMS component of SAM, and a Picarro Cavity Ring Down CO_2 Isotope Analyzer (hereafter referred to as the CRDS, Fig. 2), represented the TLS component of SAM (McAdam et al., 2011; Stern et al., 2011). The Picarro Cavity Ring Down CO_2 Isotopic Analyzer is a commercial instrument designed to continuously monitor atmospheric concentrations of CO_2 at atmospheric pressure. The precision for the $\delta^{13}\text{C}$ measurement of ambient CO_2 (1- σ precision is $<0.3\text{‰}$ during over a 1 h window) is analogous to that of the Tunable Laser Spectrometer (TLS) on SAM (Webster and Mahaffy, 2011). An InXitu Terra instrument, a portable version of the CheMin XRD/XRF instrument developed for use in the field (Blake,

2010) was used to obtain bulk mineralogy of samples. All measurements were made in a temporary remote laboratory set up in Ny Ålesund. $\delta^{13}\text{C}$ measurements on an isotope ratio mass spectrometer (IRMS) were done at the Carnegie Institution of Washington and NASA Goddard Space Flight Center.

2.2.1. Terra XRD/XRF

Several iterations of field portable CheMin prototypes have been deployed during past AMASE campaigns (Bish et al., 2007). Mini-CheMin was the first portable XRD/XRF system with both the hardware and software necessary to make mineralogical analysis quickly and efficiently in the field (Blake, 2010). A commercial XRD/XRF instrument based on the mini-CheMin platform, called Terra (<http://www.inxitu.com/html/Terra.html>), was developed by InXitu, Inc. (Blake, 2010). A Terra XRD/XRF instrument was used during the AMASE 2010 campaign to measure bulk mineralogy of fine grained ($<150\text{ }\mu\text{m}$) powders or fractions of analog samples. Terra uses $\text{Co K}\alpha$ radiation and produces XRD patterns with a 2θ range of $2\text{--}55^\circ$ and a 2θ resolution of 0.25° FWHM. The XRF energy range is $3\text{--}25\text{ keV}$ with an energy resolution of 200 eV at 5.9 keV . Terra has been shown to produce XRD data comparable in quality with laboratory XRD data (Treiman et al., 2010). Mineral identifications were determined by comparison of measured XRD patterns with standard patterns in the ICDD database, and mineral

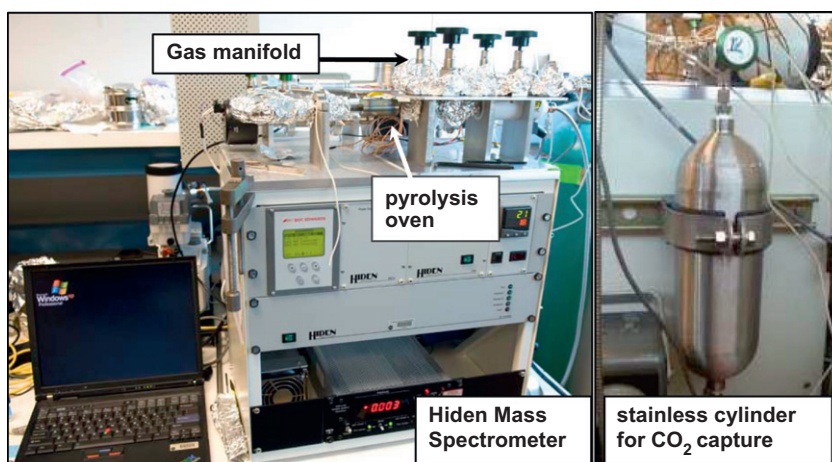


Fig. 1. Hiden Analytical HPR-20 quadrupole mass spectrometer system with pyrolysis oven and manifold (left). Side view of Hiden (right), cylinder attaches to manifold to capture CO_2 thermally evolved from carbonates.

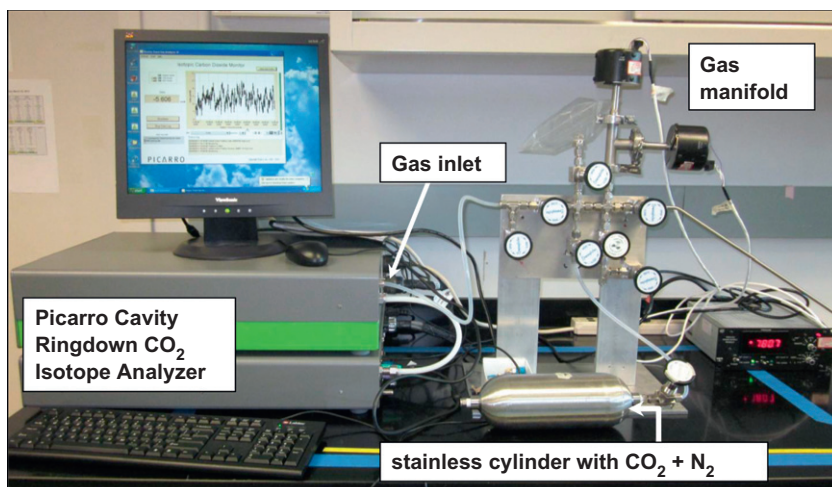


Fig. 2. Picarro Cavity Ring Down CO_2 isotope analyzer with custom manifold to introduce CO_2 evolved from carbonates.

abundances were derived by Rietveld refinement (e.g., Bish and Post, 1993; Chipera and Bish, 2002). The InXitu Terra has a minimum detection limit of 1 wt% (Treiman et al., 2010), although it may be considerably larger for poorly ordered (e.g., clay minerals) and amorphous materials (Blake, 2010; Blake et al., 2010, 2009).

2.2.2. EGA-QMS

The composition of evolved gases and the temperature of gas evolution can provide additional constraints on sample mineralogy and organic chemical characteristics. After initial analysis by Terra of a separate sample split, 5–10 mg of sample was loaded into the EGA-MS pyrolysis oven and helium carrier gas pressures and gas flow conditions similar to SAM (~ 0.027 atm-cc/sec) were established (McAdam et al., 2011). The sample was then heated from ~ 50 °C to ~ 950 °C at a ramp rate of 20 °C/min and evolved gases were monitored by the QMS. The QMS mass range is 1–300 Da, but a “peak hopping” mode was utilized, in which several Da values of interest were monitored to achieve higher time sampling. Key Da values monitored were 45 (indicating CO₂ detection), 20 (water detection), 66 (SO₂ detection), 78 (organic, benzene, fragment detection), 39 and 41 (organic, alkane, fragment detection), and 15 (methane detection).

2.2.3. EGA-CRDS

For EGA-CRDS runs, mass 45 was monitored for the onset of peaks in CO₂ evolution resulting from carbonate decomposition; the temperature at which this peak onset occurs is dependent on carbonate mineralogy. EGA-CRDS runs took place after EGA-QMS runs of the same sample, where peak onset temperature was determined and a semi-quantitative assessment of how much CO₂ was generated by EGA of the sample was made. During EGA-CRDS runs, upon mass 45 peak onset, a valve to an evacuated 1 L cylinder was opened and CO₂ was captured as it was evolved from the sample, then subsequently backfilled with N₂ to 1–2 bar to obtain CO₂ concentration and gas mixture pressure in the operating range of the Picarro CRDS (e.g. ~ 1 bar, 250–1000 ppm CO₂ in air). In the field, semi-quantitative assessment of CO₂ concentration in the 1 L cylinder was based on peak height and area of the mass 45 trace produced during EGA-QMS compared to runs with 4 mg pure calcite standard, and Terra data on carbonate concentration of a given sample. A Valedyne gauge and Baritron gauges also monitored system pressure. This information allowed determination of the appropriate amount of N₂ to backfill the tank achieve CO₂ concentrations within the Picarro operating range of 250–1000 ppm. Because nitrogen was used as the balance gas (due to availability at the field site), and the Picarro unit is factory calibrated for CO₂ in zero air (air purified to remove CO₂ and hydrocarbons), all samples were calibrated against CO₂ generated by EGA of a calcite standard of known isotopic composition and a gas mixture standard comprised of 500 ppm CO₂ in N₂.

The filled cylinder was moved from the Hiden manifold to the CRDS manifold, which had been purged with N₂ and evacuated. Occasionally, a sample produced CO₂ in concentrations exceeding the operational limits of the Picarro CRDS. In these cases, expansion into an additional volume and addition of N₂ to dilute the CO₂ concentration was necessary. Before introducing gas to the Picarro CRDS, the cylinder was opened into the manifold and gas flowed into a Teflon gas-sampling bag (Jensen Inert Products). When the pressure in the manifold equalized, the valve to the CRDS was opened and gas flowed from the bag into the CRDS at constant pressure of 1 bar. $\delta^{13}\text{C}$ measurements using this method were taken after 2 min of sample equilibration, and averaged over 5 min, and generally had 1- σ precision of 2‰ or better.

Commercial benchtop Cavity Ring Down Spectroscopy (CRDS) instrumentation for carbon isotopic analysis has become readily

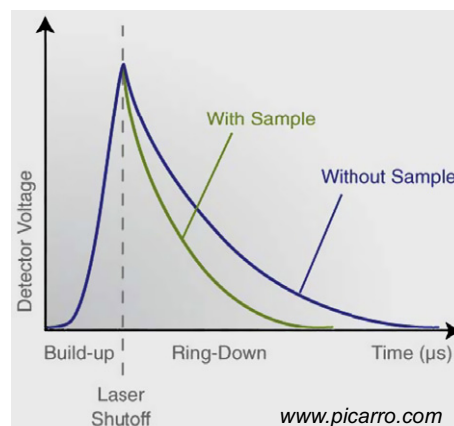


Fig. 3. Cavity Ring Down Spectrometers (CRDSs) measure the decay of light in the presence and absence of a gas of interest and translate this to gas concentration (figure used with permission from www.picarro.com). (For interpretation of the references to color in this figure legend, the reader is referred to the web version of this article.)

available in the past 5 years. These commercial CRDS CO₂ isotope analyzers (e.g., Picarro, Los Gatos Research) are designed to measure the concentration and isotopic composition of atmospheric CO₂. Briefly, CRDS measures the rate of decay of light intensity of a laser beam inside a cavity in the absence and presence of gas of interest (Fig. 3). The decay constant, or ring-down time, τ , describes the optical losses due to cavity mirrors and absorption and scattering of the sample gas, and translates into concentration measurements of gas species with absorbances in the chosen wavelength range (Crosson, 2008; Paldus and Kachanov, 2005).

While the CRDS is an approximation of the ability of TLS to measure the concentration and $\delta^{13}\text{C}$ of CO₂, the two instruments have different operational ranges. The TLS on SAM is a flight instrument designed to measure small concentrations of gas at lower pressures, and therefore does not require any backfilling steps. If too much gas is produced during an SAM-EGA-TLS experiment on Mars, it can be pumped out of the TLS Herriot Cell to reduce the pressure to optimize the measurement. Despite these differences, our system provides a way to measure $\delta^{13}\text{C}$ of samples in remote settings using absorption spectroscopy-based methods similar to the TLS on SAM.

2.3. Isotope ratio mass spectrometry (IRMS)

To ground truth EGA-CRDS isotopic measurements, isotope ratio mass spectrometry (IRMS) was performed at the Geophysical Laboratory at Carnegie Institute of Washington. Powdered samples were analyzed via acid dissolution on a Thermo Finnegan Gas Bench II coupled to a Thermo Quest Finnigan Delta Plus XL IRMS and by combustion on a Carlo Erba NC 2500 Elemental Analyzer (EA) coupled to a Thermo Scientific Delta V Plus. The values for each gas bench sample represent an average of seven aliquots of headspace CO₂ with standard deviations of ~ 0.4 ‰ ($n = 7$) for both carbon and oxygen. Precision for EA-IRMS measurements is based on reproducibility of NIST standards NBS-18, NBS-19, and Iso-Analytic standard RO22, giving typical 1- σ of ~ 0.25 ‰.

Although our field system did not enable measurement of $\delta^{18}\text{O}$ in CO₂ evolved from carbonates, the SAM flight unit will have this capability. Thus, we report $\delta^{18}\text{O}$ values obtained after the field campaign by gas bench-IRMS, bearing in mind that the SAM TLS flight instrument is capable of precisions of 3‰ for $\delta^{18}\text{O}$ in CO₂ (Webster and Mahaffy, 2011). Both carbon and oxygen isotopic values are reported relative to Pee Dee Belemnite (PDB).

3. Results

3.1. Bulk mineralogy

An array of contextual samples from each field site (Fig. 4) was analyzed for mineralogy and elemental content by Terra. Results show that the mineralogy of Knorringfjell samples is dominated by low to mid Mg-calcite, with some quartz and dolomite, whereas the Sigurdfjell carbonate samples are predominantly dolomite or aragonite (Table 2). XRD patterns acquired from the Knorringfjell green mudstone lithology (AM10-05-GM) and the Sigurdfjell surface carbonate crust (AM10-05-CS), are shown in Fig. 5a and b. These patterns illustrate the overall differences in carbonate mineralogy between the two sites, with the Knorringfjell green lithology dominated by calcite and the Sigurdfjell surface carbonate crust dominated by dolomite, and show quality of data that can be obtained with the Terra instrument. This difference in carbonate mineralogy can be attributed to differences between the characteristics of the depositional environment recorded in the Upper Jurassic/Cretaceous shallow marine carbonates at Knorringfjell and the carbonates precipitated in the Quaternary hydrothermal system associated with the subglacial basaltic volcanism at Sigurdfjell.

Knorringfjell samples are generally low to mid-Mg calcite carbonates, but some dolomite is present, particularly in the black mudstone lithology (AM10-05-BM). This is consistent with the findings of other groups who have studied this site, who find trace dolomite inside peloids thought to be associated with localized bacterial fermentation of organic matter below the sulfate reduction zone (Hammer et al., 2011). Also notable is ~20% muscovite in the green mudstone lithology. We did not see evidence of phyllosilicate decomposition in the 20 Da (H₂O) EGA-QMS trace from this sample, but this could be due to our relatively high H₂O background during this sample run in the field and/or some differences in mineralogy between the split of sample provided to the CheMin team vs. the split provided to the SAM team.

The composition of Sigurdfjell samples reflected minerals associated with basaltic igneous rocks. Sample AM10-23-B was characterized by augite, fosteritic olivine, and Na–Ca plagioclase, consistent with basalt. Some trace Mg-calcite and dolomite were detectable, as vesicles in basalt had been filled with carbonate cements. It is interesting to note that the carbonate crust, or rind, had detectable variations from the carbonate/basalt interface (AM10-27-CB) to the surface of the carbonate crust (AM10-27-CS). Internal carbonates (AM10-27-CI) were distinctively more aragonite rich (76% aragonite, 21% dolomite) than either the carbonate/basalt interface (66% dolomite, 5% aragonite, 5% low Mg-calcite) or the exterior surface of the carbonate crust (95% dolomite, 1% aragonite). As these samples were collected by dremelling each layer,

Table 2

Bulk mineralogy and qualitative elemental data from Terra XRD/XRF.

Sample ID	Sample description	Terra XRD
<i>Knorringfjell</i>		
AM10-05-GM	Green mudstone, outside	70% Mg-calcite 19% Muscovite 11% Quartz
AM10-05-WL	White crystalline	99% Low-Mg-calcite 1% Dolomite
AM10-05-BM	Black mudstone, interior	94% Low-Mg calcite 6% Dolomite
AM10-13-M	Black micrite, exterior	81% Calcite 19% Quartz
<i>Sigurdfjell</i>		
AM10-27-CB	Carbonate/basalt interface	66% Dolomite 13% Augite 7% Plagioclase 5% Aragonite 4% Goethite 5% Low-Mg-calcite
AM10-27-CS	Surface of carbonate crust	95% Dolomite 3% Goethite 1% Aragonite 1% Mg-calcite
AM10-27-CI	Internal carbonate	76% Aragonite 21% Dolomite 1% Calcite 3% Goethite
AM10-27-B	Basalt	44% Augite 27% Fe-forsterite 26% Na–Ca plagioclase 2% Biotite Trace Mg calcite and dolomite

spatial resolution was not high, but approximated what could be achieved on a robotic rover. Nonetheless, sample heterogeneity is not a sufficient explanation for the gradation in carbonate mineralogy. Finally, all 3 carbonate samples had 3–4% goethite, which is consistent with basalt weathering.

3.2. Evolved Gas Analysis

Because of the limitations of time and resources during the field study, which was meant to impose limitations similar to those encountered on a Mars rover, four samples from Knorringfjell and four samples from Sigurdfjell were analyzed by EGA-QMS with the Hiden Mass Spectrometer (Fig. 4). Carbon isotopic data was collected via EGA-CRDS for all but one basalt sample from Sigurdfjell, which had insufficient inorganic carbon for analysis.



Fig. 4. Left: Knorringfjell sample with (a) black mudstone (AM10-05-BM), (b) green mudstone (AM10-05-GM), and (c) white lithology (AM10-05-WL). Middle: (d) Micrite (AM10-13-M) sample from Knorringfjell. Right: Sigurdfjell sample with (e) external carbonate crust (AM10-27-CS), (f) internal carbonate (AM10-27-CI), (g) carbonate/basalt interface cement (AM10-27-CB), and (h) basalt (AM10-27-B). (For interpretation of the references to color in this figure legend, the reader is referred to the web version of this article.)

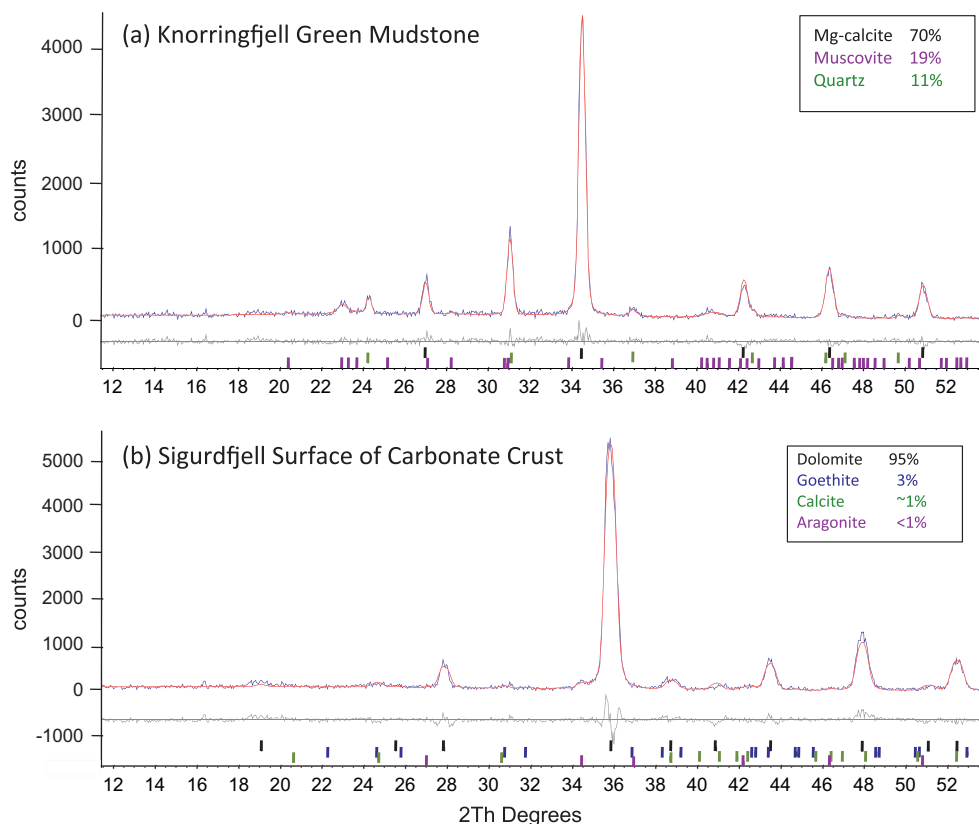


Fig. 5. Original XRD data are in blue, the simulated pattern is in red, the difference curve is in black, and the positions of all possible X-ray reflections are shown at the bottom of the pattern, color coded to the phases listed. (a) Diffraction pattern and Rietveld refinement results for the Knorringfjell green lithology. (b) Diffraction pattern and Rietveld refinement results for the Sigurdfjell exterior carbonate layer. Note the offset of the major peak, representing the difference between the mineralogy of the major carbonate phases. (For interpretation of the references to color in this figure legend, the reader is referred to the web version of this article.)

Evolved gas analysis of Knorringfjell carbonates show a diversity of organic carbon compounds, as well as the complexity of the mineralogy. Knorringfjell carbonates evolved organics over a wide range of temperatures, possibly indicating a range of thermal

maturity or difference in binding to the rock matrix. The green mudstone (AM10-05-GM), in particular showed evolution of alkane fragments at a broad distribution of temperatures, as well as benzene (Fig. 6). Tentative identification of methane trapped

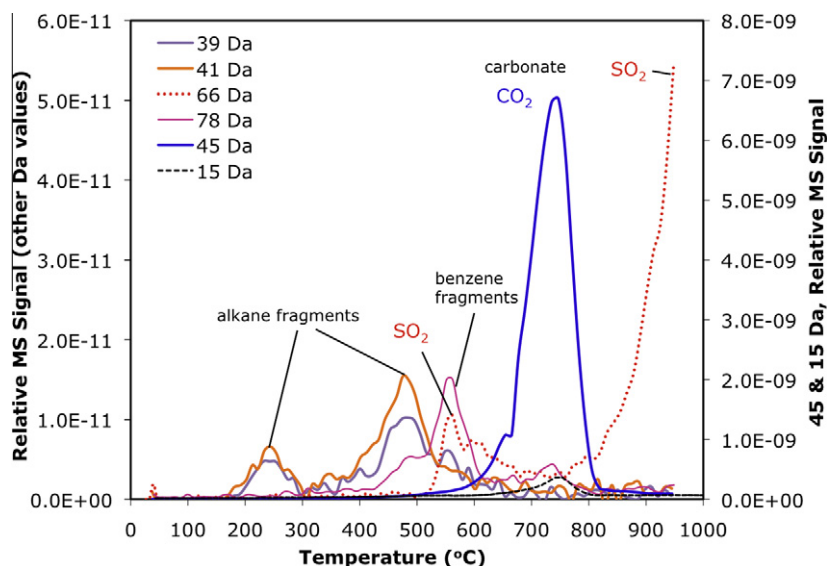


Fig. 6. EGA traces from the green carbonate lithology from Knorringfjell. The peak in the 45 Da trace is consistent with carbonate. The 39 and 41 Da traces and the 78 trace indicate the presence of alkane fragments and benzene fragments, respectively. The low temperature peak in the 66 Da trace (~560 °C) is consistent with SO₂ evolution during pyrolysis of pyrite, which has been found in micrites associated with Knorringfjell Seep Carbonates by Hammer et al. (2011). (For interpretation of the references to color in this figure legend, the reader is referred to the web version of this article.)

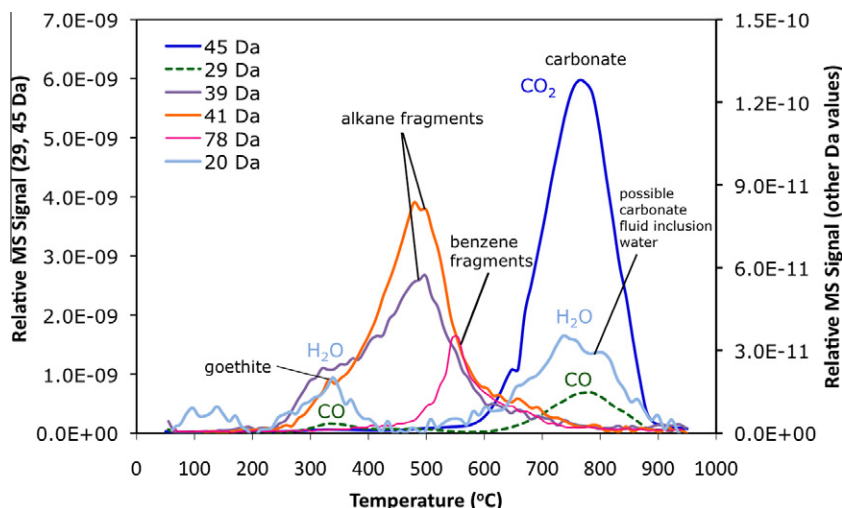


Fig. 7. EGA traces from the surface of the Sigurdffjell carbonate crust. The 45 Da peak occurs at a temperature consistent with the thermal decomposition of the dolomite known from Terra XRD results to comprise the majority of the sample's carbonate mineralogy. The low-temperature 29 Da peak may result from partial oxidation of organics to CO by H₂O released by goethite at that pyrolysis temperature. The 39 and 41 Da traces indicate the presence of alkane fragments and benzene fragments, respectively. (For interpretation of the references to color in this figure legend, the reader is referred to the web version of this article.)

within the carbonate in this sample was also made, based on coincident peaks in the 15 Da and 45 Da EGA-QMS traces from this sample with peaks between 700 and 800 °C (Fig. 6). It is unclear as to whether this methane is trapped in the carbonate or methane made as a by-product of pyrolyzing organics. In addition, the 66 Da trace from the EGA-QMS analyses showed a low temperature SO₂ peak evolving between 500 and 600 °C consistent with SO₂ evolved from laboratory EGA of pyrite samples. This suggests trace amounts of pyrite in these rocks. The 66 Da trace peak starting at around 800 °C (and continuing beyond the length of the run) is consistent with the SO₂ peak onset temperature observed during laboratory analysis of some Mg- or Ca-sulfates (e.g., epsomite). We interpret these SO₂ features as possible indications of pyrite and Mg- or Ca-sulfate as trace minerals present as less than 1% of the mineral matrix because they are below the Terra's limit of detection. It should be noted that other studies of this site have reported detection of pyrite associated with these carbonates (Hammer et al., 2011).

EGA of carbonates and basalts from Sigurdffjell reflect the presence of organics on the surface crust of the carbonate as well as in the basalt (Fig. 7). In some sample traces (AM10-27-CS), a distinct low temperature CO (29 Da) peak is seen, possibly a product of the oxidation of organics during heating in the presence of water from hydrated minerals (e.g., goethite). This hypothesis is supported by the low-temperature evolution of H₂O coincident with CO (Fig. 7). The peak in the 45 Da trace occurs at a temperature consistent with the thermal decomposition of the dolomite, known from Terra XRD

results to comprise the majority of the sample's carbonate mineralogy. Without Terra results, it would probably be difficult to discern the presence of dominant dolomite vs. dominant calcite. EGA-QMS would likely be unable to discriminate between these two particular carbonate minerals based on the peaks in the 45 Da EGA-QMS traces alone, because the decomposition temperatures of calcite and dolomite are similar. Siderite and magnesite, however, decompose at lower temperatures than those of calcite and dolomite and would be discernable from calcite and dolomite through EGA.

3.3. Stable isotopes

$\delta^{13}\text{C}$ values from Cavity Ring Down measurements are shown in Table 3. Measurements are comparable to those obtained by conventional combustion elemental analysis (EA) and gas bench IRMS. A few CRDS values deviated significantly from IRMS values or had large standard deviations; these measurements represent cases when the sample was too dilute, and the CO₂ concentration was on the very edge of the analytical window of the instrumentation. These samples were run again upon returning to the laboratory at GSFC.

$\delta^{13}\text{C}$ measurements by EGA-CRDS had larger error than IRMS measurements, but despite this, they track reasonably well (within ~3‰) with IRMS measurements, though CRDS measurements are generally less precise with 1- σ errors of 2–4‰. CRDS measurements were more precise with the carbon-enriched samples ($C > 7\%$), which provided good signal to noise ratios and 1- σ errors

Table 3
Stable carbon and oxygen isotopic data for Knorringfjell and Sigurdffjell samples.

Sample ID	Sample description	% C EA/delta V	$\delta^{13}\text{C}$ ‰ (PDB) EA/delta V	$\delta^{13}\text{C}$ ‰ (PDB) EGA/CRDS	$\delta^{13}\text{C}$ ‰ (PDB) Gas bench/delta XL	$\delta^{18}\text{O}$ ‰ (PDB) Gas bench/delta XL
<i>Knorringfjell</i>						
AM10-05-GM	Green mudstone	8.40	−39.3	−42.6	−38.8	−0.6
AM10-05-WL	White crystalline	7.92	−18.7	−18.6	−19.1	−14.8
AM10-05-BM	Black mudstone	11.84	−35.1	−38.8	−34.7	−6.2
AM10-13-M	Black micrite	8.67	−35.2	−34.5	−35.6	−0.6
<i>Sigurdffjell</i>						
AM10-27-CB	Carbonate/basalt interface	0.55	−1.3	0.9	1.6	−16.3
AM10-27-CS	Surface carbonate crust	10.36	2.3	0.7	2.1	−16.9
AM10-27-CI	Internal carbonate	11.22	0.9	−2.8	0.8	−22.1
AM10-23-B	Basalt	0.8	−5.3	NA	0.5	−15.9
AM10-23-WB	Weathered Basalt	0.69	−5.9	NA	1.9	−15.9

below 2‰. The agreement between values obtained by EGA-CRDS, which should access primarily inorganic $\delta^{13}\text{C}$ (e.g. carbonates), and EA-IRMS, a bulk combustion method that measures both organic and inorganic $\delta^{13}\text{C}$, indicate that these samples have only very trace amounts of organic carbon. The agreement of EGA-CRDS $\delta^{13}\text{C}$ with Gas Bench-IRMS data, which only measures $\delta^{13}\text{C}$ of carbonates in the sample, is further indication that there was a minimal contribution of any oxidized organic carbon to the $\delta^{13}\text{C}$ value.

Carbon isotope analysis of three of the Knorringfjell samples reveals ^{13}C -depleted values of -30‰ to -40‰ , with the exception of the white crystalline lithology (AM10-05-WL) identified by Terra as 99% calcite, which has $\delta^{13}\text{C}$ of -19‰ . Sigurdfjell samples are dramatically different, with $\delta^{13}\text{C}$ values all near 0‰ . Additional data collected for vent carbonate samples at this site have $\delta^{13}\text{C}$ of -5‰ (Table 3, AM10-0023).

$\delta^{18}\text{O}$ values of CO_2 evolved during acid dissolution of carbonates during Gas Bench – IRMS measurements are also presented in Table 3. Although we did not have the capability to make this measurement in the field, the SAM-TLS experiments will make $\delta^{18}\text{O}$ measurements of CO_2 evolved from carbonates with precisions of $\sim 3\text{‰}$ (Webster and Mahaffy, 2011). Again, Knorringfjell samples are isotopically distinct from Sigurdfjell samples. The white lithology stands alone, with $\delta^{18}\text{O} = -14.8\text{‰}$, closer to Sigurdfjell samples than Knorringfjell.

4. Discussion

Although carbon isotopic composition alone cannot determine biogenicity of a sample, it can, in the context of other geochemical, mineralogical, and environmental evidence, provide very strong evidence for the products of biological processes. Isotope results obtained using EGA-CRDS with our customized system are sufficiently precise to resolve $\delta^{13}\text{C}$ variations on the order of 3–5‰. This resolution was sufficient to show differences in carbon sources between the two sites. At 2‰ precision, the flight instrument TLS has even better precision for $\delta^{13}\text{C}$ measurements (Webster and Mahaffy, 2011).

In the case of the Knorringfjell methane seep, which has been studied in detail by Norwegian paleontologists (Hammer et al., 2011), several lines of evidence suggesting biological activity were well within the capabilities of MSL or a similarly equipped rover to detect. First, the macrofossils in these hand samples were clearly visible. Mineralogy and geochemistry from evolved gas analysis established the presence of reduced organics, including ubiquitous alkanes, the possible presence of reducing minerals (e.g. pyrite), and tentative detection of methane (which the SAM TLS would also be capable of identifying to verify mass spectrometric identification by QMS). The ^{13}C depleted isotopic values of these carbonates is consistent with their formation as authigenic carbonate units, precipitated above an active chemosynthetic community metabolizing methane as an energy source. Active methane cold seeps on Earth have been found to have rich bacterial diversity, based on the ability of sulfate reducing *Archaea* to mediate anaerobic methane oxidation (AOM) and to generate intermediate ^{13}C depleted carbon sources (e.g. formate or acetate) for nonmethanotrophic microbes (Orphan et al., 2002). Although the presence of pyrite alone is insufficient to indicate AOM or even sulfate reducing bacteria (SRB), the taxa identified by Hammer et al. (2011) at this site have been linked to sulfide formation via anaerobic oxidation of methane, including vestimentiferans, solemyids, and lucinids, all of which have sulfide-oxidizing bacterial symbionts (Dubilier et al., 2008). Furthermore, tentative detection of an Mg- or Ca-sulfate mineral by EGA-QMS may be consistent with competing sulfide-oxidizing bacteria within the community, or oxidation of reduced sulfur materials in more oxygenated waters (Kuenen

et al., 1985). Sulfide-oxidizing bacteria depend on the presence of reduced sulfur, and are therefore found in settings where bacterial sulfate reduction takes place or where an inorganic source of reduced sulfur is available (e.g. Kuenen et al., 1985). Similar isotopic anomalies of ^{13}C -depleted carbonates associated with methane seeps have been found in the Canadian Arctic and the Gulf of Mexico (Beauchamp et al., 1989), although in some cases a range of ^{13}C values may exist at a single seep due to the presence of complex carbon sources (Campbell et al., 2002; Roberts and Aharon, 1994). Our observations are consistent with other stable carbon isotopic studies at this site (Fig. 8), where micrites and calcite spar were moderately depleted ($\delta^{13}\text{C} = -15\text{‰}$ to -23‰ VPDB) and wackestone phases (e.g. black and green carbonate lithologies) were variable, but more depleted than the micrite or calcite spar, with $\delta^{13}\text{C}$ as low as -43‰ (Hammer et al., 2011; Nakrem et al., 2010).

The presence of the white calcite lithology (AM10-05-WL) inside an apparent vug and/or vein within the rock suggest that this phase was formed later than the mudstone and micritic lithologies. The ^{18}O depletion of this calcite with respect to the mudstone and micrite lithologies suggests formation associated with hydrothermal fluid temperatures up to 130°C (Hammer et al., 2011). This sample appears to be representative of the sparite (coarsely crystalline calcite cement) phase filling fractures and veins identified by Hammer et al. (2011), which are thought to have formed via hydrothermal activity during a burial event associated with the High Arctic Large Igneous Province (Maher, 2001).

In general, carbonates at Knorringfjell are isotopically distinct from those measured in carbonate/basalt breccia crusts from Sigurdfjell (Fig. 8). Additionally, the mineralogy of Sigurdfjell samples reflects mafic igneous materials (e.g. anorthite and augite) accompanied by common basalt weathering products such as goethite. The carbonate mineralogy of the Sigurdfjell samples is also distinct from that of Knorringfjell; very low amounts of calcite are present in Sigurdfjell carbonates, which are dominated by dolomite and

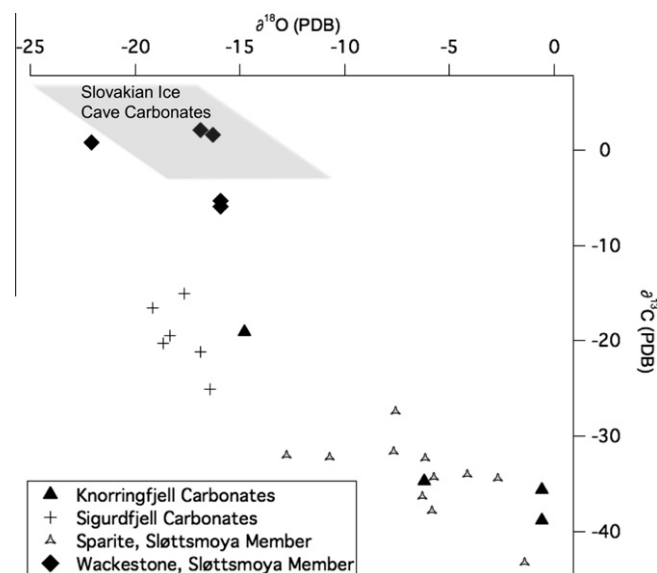


Fig. 8. $\delta^{13}\text{C}$ and $\delta^{18}\text{O}$ values of carbonates in this study (filled diamonds and triangles), compared with isotopic values measured in the Sløttsmoya Member (crosses and open triangles) by Hammer et al. (2011) and cryogenic carbonates in Slovakian ice caves from Zak et al. (2004). The isotopic values of the Slovakian cryogenic carbonates show similarities to Sigurdfjell carbonates, and the isotope values of Knorringfjell carbonates from this study overlap with the range of values obtained from Knorringfjell carbonates by Hammer et al. (2011).

aragonite. This difference in carbonate mineralogy can be attributed to differences in the characteristics of the two distinct depositional environments, such as differences in the fluid compositions and age of the rocks. At Sigurd fjell, fluids from which the carbonates precipitated would have more abundant Mg in solution as compared with Knorring fjell, due to their widespread interaction with the mafic basalt materials. This could be responsible for more prevalent dolomite at Sigurd fjell.

Although precipitation from hydrothermal fluids has been proposed for the origin of Sigurd fjell carbonate, (Steele et al., 2007; Treiman et al., 2002), it has recently been noted (Amundsen et al., 2011) that Sigurd fjell and other Bockfjorden Volcanic Complex (BVC) lava-hosted carbonates are isotopically similar to cave carbonates formed cryogenically via slow freezing of water, CO₂ outgassing from solution, and partial water evaporation Fig. 8. Similar observations have been noted for Arctic carbonate crusts on Ellesmere Island (Socki et al., 2009) and for carbonate globules formed under laboratory cryogenic conditions (Niles et al., 2004). Carbonates are precipitated during slow freezing in isotopic equilibrium with surrounding glacial melt, with limited CO₂ outgassing and low $\delta^{18}\text{O}$ values resulting from Rayleigh fractionation between ice and residual solution (Zak et al., 2004). In this scenario, subglacial eruption of CO₂-rich magmas would have melted the surrounding glacial ice, followed by cryogenic carbonate precipitation characterized by progressive ^{18}O depletion during closed-system freezing (Zak et al., 2004). Similar processes have been described associated with aufeis formation in the Arctic (Clark and Lauriol, 1997; Lacelle et al., 2006), where cryogenic carbonate precipitation may happen without communication with the atmosphere, and results in carbonate with very low $\delta^{18}\text{O}$ values between -24‰ and -32‰ (PDB).

At Sigurd fjell, the origin of the CO₂ is not entirely clear and $\delta^{13}\text{C}$ values may represent a mixing of the isotopic signature of meteoric CO₂ in glacial ice and mantle-derived CO₂. Basalt samples taken from other vents on Sigurd fjell have bulk $\delta^{13}\text{C}$ values of $\sim -5.6\text{‰}$ (Table 3, AM10-23-B, AM10-23-WB), consistent with mantle carbon. However, analysis of only the carbonate component of these samples gives near-zero $\delta^{13}\text{C}$ values. Alternatively, the source of the CO₂ could have been mantle outgassing, but the kinetic isotope effect associated with rapid outgassing of CO₂ from solution during rapid freezing of ice, causing ^{13}C enrichment in residual fluid, would have erased the original mantle values. To further complicate interpretation, subsequent low-temperature hydrothermal alteration of these carbonates, may have also changed the isotopic signatures encoded during the original precipitation event (Amundsen, 1987; Treiman et al., 2002).

Both cryogenic (Amundsen et al., 2011; Niles et al., 2004; Socki et al., 2009) and hydrothermal (Niles et al., 2005; Steele et al., 2007) origins for martian meteorite ALH84001 carbonates have been suggested. Alternatively, recent clumped isotope geothermometry of ALH84001 carbonates suggests the formation of these carbonates at $18 \pm 4^\circ\text{C}$ (Halevy et al., 2011). These recent data, coupled with iron microprobe observations of core-to-rim enrichment in ^{18}O and ^{13}C of ALH84001 carbonates (e.g., Leshin et al., 1998; Niles et al., 2005), is used to support a scenario for slow precipitation of carbonates under isotopic equilibrium in a partially closed environment where fluids had limited exchange with the atmosphere. The suggested mechanism involves gradual evaporation driving loss of the lighter isotopes to CO₂ and water vapor, enriching residual fluids and resulting in isotopic zonation of carbonates (Halevy et al., 2011). Applying clumped isotope geothermometry to BVC carbonates would help resolve the water temperature at the time of carbonate precipitation, and better spatial carbon and oxygen isotopic resolution of zoned carbonates in basalts and carbonate crusts on basaltic vents would elucidate their formation histories.

4.1. Relevance to MSL and Mars

Our study suggests that this subset of instrumentation, which represents a fraction of the analytical toolset on Mars Science Laboratory, can make several fundamental measurements on Mars with resolutions comparable to those made in our field exercises. Terra was able to resolve differences in carbonate mineralogy that were inconclusive from EGA-QMS data alone. Conversely, EGA-QMS was capable of detecting trace amounts of sulfur phases that Terra did not see. It is expected that SAM and CheMin will complement one another in this way during MSL operations on Mars. EGA-QMS detected a suite of organics that evolved across a wide temperature range. EGA-QMS also detected evolved SO₂ consistent with SO₂ evolution temperatures for both reduced and oxidized sulfur minerals. Finally, the isotopic data obtained by evolving CO₂ from carbonates using a commercial Picarro Cavity Ring Down CO₂ isotope analyzer as a proxy for the SAM-TLS were successful in identifying signatures of carbon from two very different sources when combined with geochemical data from Terra and EGA-QMS.

MSL, and SAM in particular, will have additional tools at its disposal not represented in this study, including the ability to combust reduced organics to CO₂ and analyze their $^{13}\text{C}/^{12}\text{C}$ ratios, and the ability to determine concentration and $\delta^{13}\text{C}$ of methane both in the atmosphere and evolved from samples. Organics detection on SAM will be further enhanced by gas chromatography columns, trapping of organics, and even a derivatization experiment Mahaffy et al., 2012. Additionally, concentration, D/H, and $^{18}\text{O}/^{16}\text{O}$ measurements of H₂O evolved from samples will complement CheMin mineralogical analyses of clays. Though these capabilities are beyond the scope of this field study, they will offer a more sophisticated and thorough analysis of gases evolved from Mars regolith during the MSL mission.

Martian carbonate precipitation could have occurred via multiple mechanisms, including hydrothermal, cryogenic, or evaporative deposition. Orbital data showing carbonate cements and breccias associated with large impact basins support the notion of hydrothermal carbonate formation. Volcanic intrusion into ice, similar to the subglacial BVC in Svalbard, could lead to one of several possible environments analogous to carbonate precipitation on Mars. The large amount of water ice, thought to exist just below the surface in some regions on Mars (e.g., Byrne et al., 2009; Holt et al., 2008; Smith et al., 2009) could easily be melted by volcanism or heat generated by impact on the martian surface (Parnell et al., 2010). This water could provide solutions for hydrothermal carbonate precipitation, as well as cryogenic formation of carbonates in cooler areas along the margins of hydrothermal systems. Evaporative precipitation of carbonates during a past time of warmer average surface temperatures cannot be excluded, in light of the recently suggested $\sim 18^\circ\text{C}$ formation temperatures for the ancient carbonates in ALH84001 (Halevy et al., 2011). Although large carbonate deposits have not been identified on the martian surface, carbonates have been inferred to be present in some surface areas (e.g., Ehlmann et al., 2008; Michalski and Niles, 2010) and in martian dust (e.g., Bandfield et al., 2003) through orbital spectroscopic observations, detected in the Comanche outcrop at Gusev Crater by the MER Spirit Rover (Morris et al., 2010), and found in abundances of several weight percent in regolith at the Phoenix landing site (Boynton et al., 2009). Analog studies highlighting complications in using remote sensing to detect carbonates suggest that even more massive deposits may exist (Bishop et al., 2011) despite evidence that points to an acidic Mars aqueous environment in more recent geologic history. These carbonates could have been preserved by burial either by volcanism or sedimentation (Michalski and Niles, 2010) and they may provide an isotopic record of atmospheric CO₂, like carbonates in martian meteorites (Niles et al., 2005, 2009). With appropriate analytical tools, such as the techniques presented in this study, carbon and oxygen isotopic measurements of carbonates on the martian surface

could reveal a rich environmental history, and possibly, with contextual mineralogical, chemical, and morphological evidence, signatures of relict biological processes.

5. Conclusion

In this study, EGA-QMS, Terra XRD, and a Picarro CRDS were used to emulate a subset of capabilities in the analytical laboratory in the body of the MSL “Curiosity” rover. Our field instrument suite was able to detect differences in mineralogy, $\delta^{13}\text{C}$, and organics content in several samples from two different sites representing two different past Mars environments. Our data revealed two different sets of processes responsible for carbonate formation at the two sites; authigenic carbonate precipitation associated with chemosynthetic activity at a fossil methane seep, and abiotic precipitation associated with either cryogenic or hydrothermal processes. Our data suggest that cryogenic carbonate formation is a plausible origin for BVC carbonates, though more analysis, including clumped isotope geothermometry, and spatially resolved isotopic data could help better constrain formation mechanisms for these unique carbonates that provide a terrestrial analog for martian meteorite ALH84001.

Acknowledgments

The authors would like to acknowledge NASA's Astrobiology Science and Technology for Exploring Planets (ASTEP) Program for funding, the entire 2010 AMASE Team, the Ny Ålesund community, the Norwegian Polar Institute, and the European Space Agency. The authors also thank two anonymous reviewers for their helpful comments.

References

- Abramov, O., Kring, D.A., 2005. Impact-induced hydrothermal activity on early Mars. *J. Geophys. Res. – Planets* 110, 1–19.
- Amundsen, H.E.F., 1987. Evidence for liquid immiscibility in the upper mantle. *Nature* 327, 692–695.
- Amundsen, H.E.F. et al., 2010. Integrated exomars PanCam, Raman, and close-up imaging field tests on AMASE 2009. *Geophys. Res. Abstr.* 12, Abstract EGU2010-8757.
- Amundsen, H.E.F. et al., 2011. Cryogenic Origin for Mars Analog Carbonates in the Bockfjord Volcanic Complex, Svalbard (Norway). *Lunar Planet. Sci.* 42, 2223.
- Bandfield, J.L., Glotch, T.D., Christensen, P.R., 2003. Spectroscopic identification of carbonate minerals in the martian dust. *Science* 301, 1084–1087.
- Beauchamp, B., Krouse, H.R., Harrison, J.C., Nassichuk, W.W., Eliuk, L.S., 1989. Cretaceous cold-seep communities and methane-derived carbonates in the Canadian Arctic. *Science* 244, 53–56.
- Bish, D.L., Post, J.E., 1993. Quantitative mineralogical analysis using the rietveld full-pattern fitting method. *Am. Mineral.* 78, 932–940.
- Bish, D.L. et al., 2007. Field Xrd/Xrf Mineral Analysis by the Msl CheMin Instrument. *Lunar Planet. Sci.* 38, 1163.
- Bishop, J.L. et al., 2001. Mineralogical and geochemical analyses of antarctic lake sediments: A study of reflectance and Mossbauer spectroscopy and C, N, and S isotopes with applications for remote sensing on Mars. *Geochim. Cosmochim. Acta* 65, 2875–2897.
- Bishop, J.L., Schelble, R.T., McKay, C.P., Brown, A.J., Perry, K.A., 2011. Carbonate rocks in the Mojave Desert as an analogue for martian carbonates. *Int. J. Astrobiol.* 10, 349–358.
- Blake, D., 2010. A Historical Perspective of the Development of the CheMin Instrument for the Mars Science Laboratory (Msl '11) Mission. *Geochemical News*.
- Blake, D.F. et al., 2009. The CheMin Mineralogical Instrument on the Mars Science Laboratory Mission. *Lunar Planet. Sci.* 50.
- Blake, D.F. et al., 2010. Test and Delivery of the CheMin Mineralogical Instrument for Mars Science Laboratory 11. *Lunar Planet. Sci.* 41, 1898.
- Boynton, W.V. et al., 2009. Evidence for CALCIUM carbonate at the Mars Phoenix landing site. *Science* 325, 61–64.
- Byrne, S. et al., 2009. Distribution of mid-latitude ground ice on Mars from new impact craters. *Science* 325, 1674–1676.
- Campbell, K.A., Farmer, J.D., Des Marais, D., 2002. Ancient Hydrocarbon Seeps from the Mesozoic convergent margin of California: Carbonate geochemistry, fluids and palaeoenvironments. *Geofluids* 2, 63–94.
- Carr, R.H., Grady, M.M., Wright, I.P., Pillinger, C.T., 1985. Martian atmospheric carbon-dioxide and weathering products in Snc meteorites. *Nature* 314, 248–250.
- Chapman, M.G., Tanaka, K.L., 2002. Related magma, Åiice interactions: Possible origins of chasmata, chaos, and surface materials in xanthe, margaritifer, and Meridiani Terrae, Mars. *Icarus* 155, 324–339.
- Chipera, S.J., Bish, D.L., 2002. Fullpat: A full-pattern quantitative analysis program for X-ray powder diffraction using measured and calculated patterns. *J. Appl. Crystallogr.* 35, 744–749.
- Clark, I.D., Lauriol, B., 1997. Aufeis of the Firth river basin, Northern Yukon Canada: Insights into permafrost hydrogeology and Karst. *Arct. Alp. Res.* 29, 240–252.
- Crosson, E.R., 2008. A cavity ring-down analyzer for measuring atmospheric levels of methane, carbon dioxide, and water vapor. *Appl. Phys. B: Lasers Opt.* 92, 403–408.
- Dubilier, N., Bergin, C., Lott, C., 2008. Symbiotic diversity in marine animals: The art of harnessing chemosynthesis. *Nat. Rev. Microbiol.* 6, 725–740.
- Dypvik, H. et al., 1991. The Janusfjellet subgroup (Bathonian to Hauterivian) on central Spitsbergen – A revised lithostratigraphy. *Polar Res.* 9, 21–43.
- Dypvik, H., Nagy, J., Eikeland, T.A., Backerow, K., Johansen, H., 1991. Depositional conditions of the Bathonian to Hauterivian Janusfjellet subgroup, Spitsbergen. *Sediment Geol.* 72, 55–78.
- Edwards, B.R., Tuffen, H., Skilling, I.P., Wilson, L., 2009. Introduction to special issue on volcano-ice interactions on Earth and Mars: The state of the science. *J. Volcanol. Geotherm. Res.* 185, 247–250.
- Ehlmann, B.L. et al., 2008. Orbital identification of carbonate-bearing rocks on Mars. *Science* 322, 1828–1832.
- Fairen, A.G. et al., 2005. Prime candidate sites for astrobiological exploration through the hydrogeological history of Mars. *Planet. Space Sci.* 53, 1355–1375.
- Farquhar, G.D., Ehleringer, J.R., Hubick, K.T., 1989. Carbon isotope discrimination and photosynthesis. *Ann. Rev. Plant Physiol.* 40, 503–537.
- Fernandez-Remolar, D.C., Morris, R.V., Gruener, J.E., Amils, R., Knoll, A.H., 2005. The Rio Tinto basin, Spain: Mineralogy, sedimentary geobiology, and implications for interpretation of outcrop rocks at Meridiani Planum, Mars. *Earth Planet. Sci. Lett.* 240, 149–167.
- Goetz, W. et al., 2011. Mars Organic Molecule Analyzer (Moma) Field Test as Part of the AMASE 2010 Svalbard Expedition. *Lunar Planet. Sci.* 42, Abstract 2460.
- Halevy, I., Fischer, W.W., Eiler, J.M., 2011. Carbonates in the martian meteorite Allan Hills 84001 formed at $18 \pm 4^\circ\text{C}$ in a near-surface aqueous environment. *Proc. Nat. Acad. Sci.* 108, 16895–16899.
- Hamilton, C.W., Fagents, S.A., Thordarson, T., 2011. Lava and ground ice interactions in Elysium Planitia, Mars: Geomorphological and geospatial analysis of the Tartarus Colles Cone groups. *J. Geophys. Res.* 116, E03004.
- Hammer, O. et al., 2011. Hydrocarbon seeps from close to the Jurassic–Cretaceous boundary, Svalbard. *Palaeogeogr. Palaeoclimatol.* 306, 15–26.
- Hayes, J.M., 1993. Factors controlling ^{13}C contents of sedimentary organic compounds: Principles and evidence. *Mar. Geol.* 113, 111–125.
- Hoefs, J., 1980. *Stable Isotope Geochemistry*. Springer-Verlag, Heidelberg, Germany.
- Holt, J.W. et al., 2008. Radar sounding evidence for buried glaciers in the southern mid-latitudes of Mars. *Science* 322, 1235–1238.
- Huang, Y. et al., 2005. Molecular and compound-specific isotopic characterization of monocarboxylic acids in Carbonaceous meteorites. *Geochim. Cosmochim. Acta* 69, 1073–1084.
- Jakosky, B.M., 1999. Martian stable isotopes: Volatile evolution, climate change and exobiological implications. *Orig. Life Evol. Biospher.* 29, 47–57.
- Josset, J. et al., 2011. Clupi: The high-performance close-up camera system on board the 2018 exomars rover. *Geophys. Res. Abstr.* 13, Abstract EGU2011-13365.
- Jull, A.J.T., Eastoe, C.J., Cloudt, S., 1997. Isotopic composition of carbonates in the Snc meteorites, Allan Hills 84001 and Zagami. *J. Geophys. Res. – Planets* 102, 1663–1669.
- Komatsu, G., Ori, G.G., 2000. Exobiological implications of potential sedimentary deposits on Mars. *Planet. Space Sci.* 48, 1043–1052.
- Komatsu, G. et al., 2011. Roles of methane and carbon dioxide in geological processes on Mars. *Planet. Space Sci.* 59, 169–181.
- Krajewski, K.P., 2004. Carbon and oxygen isotopic survey of diagenetic carbonate deposits in the Agardhfjellet formation (Upper Jurassic), Spitsbergen: Preliminary results. *Polish Polar Res.* 25, 27–43.
- Kuenen, J.G., Robertson, L.A., Vangemeren, H., 1985. Microbial interactions among aerobic and anaerobic sulfur-oxidizing bacteria. *Adv. Microb. Ecol.* 8, 1–59.
- Lacelle, D., Lauriol, B., Clark, I.D., 2006. Effect of chemical composition of water on the oxygen-18 and carbon-13 signature preserved in cryogenic carbonates, Arctic Canada: Implications in paleoclimatic studies. *Chem. Geol.* 234, 1–16.
- Leshin, L.A., McKeegan, K.D., Carpenter, P.K., Harvey, R.P., 1998. Oxygen isotopic constraints on the genesis of carbonates from martian meteorite ALH84001. *Geochim. Cosmochim. Acta* 62, 3–13.
- Léveillé, R., 2009. Validation of astrobiology technologies and instrument operations in terrestrial analogue environments. *C. R. Palevol.* 8, 637–648.
- Mahaffy, P., 2008. Exploration of the habitability of Mars: Development of analytical protocols for measurement of organic carbon on the 2009 Mars Science Laboratory. *Space Sci. Rev.* 135, 255–268.
- Mahaffy, P.R. et al., 2012. The Sample Analysis at Mars Investigation and Instrument Suite. *Space Science Reviews*. 1–78.
- Maher, H.D.J., 2001. Manifestations of the cretaceous high arctic large Igneous Province in Svalbard. *J. Geol.* 109, 91–104.
- McAdam, A.C. et al., 2011. Field Characterization of the Mineralogy and Organic Chemistry of Carbonates from the 2010 Arctic Mars Analog Svalbard Expedition by Evolved Gas Analysis. *Lunar Planet. Sci.* 42.

- McCormoll, T.M., Seewald, J.S., 2006. Carbon isotope composition of organic compounds produced by abiotic synthesis under hydrothermal conditions. *Earth Planet. Sci. Lett.* 243, 74–84.
- Michalski, J.R., Niles, P.B., 2010. Deep crustal carbonate rocks exposed by meteor impact on Mars. *Nat. Geosci.* 3, 751–755.
- Morris, R.V. et al., 2010. Identification of carbonate-rich outcrops on Mars by the spirit rover. *Science* 329, 421–424.
- Morris, R.V. et al., 2011. A Terrestrial Analogue from Spitsbergen (Svalbard, Norway) for the Comanche Carbonate at Gusev Crater, Mars. *Lunar Planet. Sci.* 42, p. 1699 (LPI Contribution No. 1608).
- Mumma, M.J. et al., 2009. Strong release of methane on Mars in northern summer 2003. *Science* 323, 1041–1045.
- Nagy, J., Basov, V.A., 1998. Revised foraminiferal taxa and biostratigraphy of bathonian to Ryazanian deposits in Spitsbergen. *Micropaleontology* 44, 217–255.
- Nakrem, H.A., Hammer, Ø., Jørn, H., Little, C.T.S., 2010. A Hydrocarbon Seep Fauna from the Uppermost Jurassic of Spitsbergen, Svalbard. *Third International Palaeontological Congress, London*, p. 291.
- Navarro-Gonzalez, R. et al., 2003. Mars-like soils in the Atacama Desert, Chile, and the dry limit of microbial life. *Science* 302, 1018–1021.
- Navarro-Gonzalez, R. et al., 2004. Mars-like, soils in the Yungay Area, the driest core of the Atacama desert in northern Chile. In: J. Seckbach et al. (Eds.), *Life in the Universe: From the Miller Experiment to the Search for Life on Other Worlds*, pp. 211–216.
- Navarro-Gonzalez, R., Vargas, E., de la Rosa, J., Raga, A.C., McKay, C.P., 2010. Reanalysis of the viking results suggests perchlorate and organics at midlatitudes on Mars. *J. Geophys. Res. – Planets*, 115 E12, (AGU Contribution CiteID E12010).
- Niles, P.B., Leshin, L.A., Socki, R.A., Guan, Y., Ming, D.W., Gibson, E.K., 2004. Cryogenic Calcite – A Morphologic and Isotopic Analog to the ALH84001 Carbonates. *Lunar Planet. Sci.* 35, 1459.
- Niles, P.B., Leshin, L.A., Guan, Y., 2005. Microscale carbon isotope variability in ALH84001 carbonates and a discussion of possible formation environments. *Geochim. Cosmochim. Acta* 69, 2931–2944.
- Niles, P.B., Zolotov, M.Y., Leshin, L.A., 2009. Insights into the formation of Fe- and Mg-rich aqueous solutions on early Mars provided by the ALH84001 carbonates. *Earth Planet. Sci. Lett.* 286, 122–130.
- Niles, P.B., Boynton, W.V., Hoffman, J.H., Ming, D.W., Hamara, D., 2010. Stable Isotope Measurements of Martian Atmospheric CO₂ at the Phoenix Landing Site. *Science* 329, 1334–1337.
- O'Neil, J.R., 1986. Theoretical and experimental aspects of isotope fractionation. In: Valley, J.W., Taylor, Jr., H.P., O'Neil, J.R., (Eds.), *Stable Isotopes in High Temperature Geological Processes*. Rev. Mineral., pp. 1–40.
- Orphan, V.J., House, C.H., Hinrichs, K.U., McKeegan, K.D., DeLong, E.F., 2002. Multiple archaeal groups mediate methane oxidation in anoxic cold seep sediments. *Proc. Nat. Acad. Sci. USA* 99, 7663–7668.
- Paldus, B.A., Kachanov, A.A., 2005. An historical overview of cavity-enhanced methods. *Can. J. Phys.* 83, 975–999.
- Parnell, J., Mazzini, A., Honghan, C., 2002. Fluid inclusion studies of chemosynthetic carbonates: Strategy for seeking life on Mars. *Astrobiology* 2, 43–57.
- Parnell, J., Taylor, C.W., Thackrey, S., Osinski, G.R., Lee, P., 2010. Permeability data for impact breccias imply focussed hydrothermal fluid flow. *J. Geochem. Explor.* 106, 171–175.
- Committee on the Planetary Science Decadal Survey N.R.C., *Visions and Voyages for Planetary Science in the Decade 2013–2022*. 2011.
- Pondrelli, M., Rossi, A.P., Ori, G.G., van Gasselt, S., Praeg, D., Ceramicola, S., 2011. Mud volcanoes in the geologic record of Mars: The case of Firsoff crater. *Earth Planet. Sci. Lett.* 304, 511–519.
- Proskurowski, G., Lilley, M.D., Kelley, D.S., Olson, E.J., 2006. Low temperature volatile production at the lost city hydrothermal field, evidence from a hydrogen stable isotope geothermometer. *Chem. Geol.* 229, 331–343.
- Roberts, H.H., Aharon, P., 1994. Hydrocarbon-derived carbonate buildups of the northern Gulf-of-Mexico continental-slope – A review of submersible investigations. *Geo-Mar. Lett.* 14, 135–148.
- Rull, F. et al., 2011. Exomars Raman laser spectrometer for exomars. *Proc. SPIE*, 8152, p. 85120J.
- Schidlowski, M., 1992. Stable carbon isotopes: Possible clues to early life on Mars. *Adv. Space Res.* 12, 101–110.
- Schulze-Makuch, D. et al., 2007. Exploration of hydrothermal targets on Mars. *Icarus* 189, 308–324.
- Sephton, M.A., Verchovsky, A.B., Bland, P.A., Gilmour, I., Grady, M.M., Wright, I.P., 2003. Investigating the variations in carbon and nitrogen isotopes in carbonaceous chondrites. *Geochim. Cosmochim. Acta* 67, 2093–2108.
- Sherwood-Lollar, B., Lacharme-Couloume, G., Voglesonger, K., Onstott, T.C., Pratt, L.M., Slater, G.F., 2008. Isotopic signatures of CH₄ and Higher hydrocarbon gases from Precambrian shield sites: A model for abiogenic polymerization of hydrocarbons. *Geochim. Cosmochim. Acta* 72, 4778–4795.
- Skjeltkvale, B.L., Amundsen, H.E.F., Oreilly, S.Y., Griffin, W.L., Gjelsvik, T., 1989. A Primitive alkali basaltic stratovolcano and associated eruptive centers, northwestern Spitsbergen – Volcanology and tectonic significance. *J. Volcanol. Geotherm. Res.* 37, 1–19.
- Smith, P.H. et al., 2009. H₂O at the Phoenix landing site. *Science* 325, 58–61.
- Socki, R.A., Niles, P.B., Blake, W., Leveille, R., 2009. Covariant C and O Isotope Trends in Arctic Carbonate Crusts and ALH84001: Potential Biomarker or Indicator of Cryogenic Formation Environment? *Lunar Planet. Sci.* 40, 2218.
- Steele, A. et al., 2007. Comprehensive imaging and Raman spectroscopy of carbonate globules from martian meteorite ALH84001 and a terrestrial analogue from Svalbard. *Meteorit. Planet. Sci.* 42, 1549–1566.
- Stern, J.C. et al., 2011. $\Delta^{13}\text{C}$ Analysis of Mars Analog Carbonates Using Evolved Gas-Cavity Ringdown Spectrometry on the 2010 Arctic Mars Analog Svalbard Expedition (AMASE). *Lunar Planet. Sci.* 42.
- ten Kate, I.L. et al., 2010. Vapor: Volatile analysis by pyrolysis of regolith; an instrument for in situ detection of water, noble gases, and organics on the Moon. *Planet. Space Sci.* 58, 1007–1017.
- Treiman, A.H., Amundsen, H.E.F., Blake, D.F., Bunch, T., 2002. Hydrothermal origin for carbonate globules in martian meteorite ALH84001: A terrestrial analogue from Spitsbergen (Norway). *Earth Planet. Sci. Lett.* 204, 323–332.
- Treiman, A.H., Robinson, K.L., Blake, D.F., Bish, D., 2010. Mineralogy determinations by CheMin Xrd, tested on ultramafic rocks (mantle xenoliths). In: *Astrobiology Science Conference 2010: Evolution and Life: Surviving Catastrophes and Extremes on Earth and Beyond*, p. 5351 (LPI Contribution No. 1538).
- Villanueva, G.L., Mumma, M.J., Novak, R.E., 2009. Strong release of methane on Mars: Evidence of biology or geology? *Geochim. Cosmochim. Acta* 73, A1384.
- Webster, C.R., 2005. Measuring methane and its isotopes (CH₄-C-12, (CH₄)-C-13, and CH₃D on the surface of Mars with *in situ* laser spectroscopy. *Appl. Opt.* 44, 1226–1235.
- Webster, C.R., Mahaffy, P.R., 2011. Determining the local abundance of martian methane and its ¹³C/¹²C and D/H isotopic ratios for comparison with related gas and soil analysis on the 2011 Mars Science Laboratory (MSL) mission. *Planet. Space Sci.* 59, 271–283.
- Wright, I.P., Grady, M.M., Pillinger, C.T., 1988. Carbon, oxygen and nitrogen isotopic compositions of possible martian weathering products in EETA 79001. *Geochimica Et Cosmochimica Acta* 52, 917–924.
- Zak, K., Urban, J., Cilek, V., Hercman, H., 2004. Cryogenic cave calcite from several central European Caves: Age, carbon and oxygen isotopes and a genetic model. *Chem. Geol.* 206, 119–136.